Synthesis and NMR Characterization of New Hyaluronan-Based NO Donors

Chiara Di Meo,[†] Donatella Capitani,[‡] Luisa Mannina,[‡,§] Enzo Brancaleoni,[‡] Devis Galesso,[⊥] Gilda De Luca,[⊥] and Vittorio Crescenzi*[,†]

Department of Chemistry, University of Rome "La Sapienza", p.le Aldo Moro 5, 00185 Rome, Italy, Institute of Chemical Methodologies, CNR, Research Area of Rome, Via Salaria Km 29,300, 00016 Monterotondo Stazione, Rome, Italy, S.T.A.A.M. Department, University of Molise, 86100 Campobasso, Italy, and Fidia Farmaceutici SpA, Via Ponte della Fabbrica 3/a, I-35031 Abano Terme, Padua, Italy

Received November 28, 2005; Revised Manuscript Received January 15, 2006

Nitric oxide (NO) and hyaluronic acid (HA), two species widely different in terms of molecular complexity and biological competence, are both known to play an important role in the wound healing process. To combine the properties of HA and NO, we synthesized new NO-donors based on hyaluronic acid derivatives exhibiting a controlled NO-release under physiological conditions (in vitro tests). Since two molecules of NO can form a covalent bond with secondary amines to yield structures, named NONO-ates, able to release NO in solution, we used spermidine bound to HA as the NO-linker. The HA−spermidine derivative was obtained by controlled HA amidation in aqueous media, activating the biopolymer carboxylate groups with a water soluble carbodiimide. The resulting derivative, soluble in water, was fully characterized by high field ^{1}H and ^{13}C NMR spectroscopy. The amount of grafting of spermidine on HA was determined by integration of suitable ^{1}H NMR signals. In addition, cross-linked derivatives of HA were synthesized by the Ugi's four-component reaction using formaldehyde, cyclohexylisocyanide, and spermidine. The HA−spermidine networks were characterized by ^{13}C CP-MAS NMR spectroscopy. The degree of cross-linking of the networks was also determined. Finally, the release of NO from the swollen hydrogels freshly saturated with NO, in contact with aqueous media, was monitored by means of UV spectrophotometric measurements.

Introduction

NO is synthesized in vivo from L-arginine by the enzymes NOS (nitric oxide synthases) that can be either in the constitutive (cNOS) or in the inducible (iNOS) form.[1] NO is a gas showing complex biological activities which, just to mention a few, include a marked influence on the cardiovascular and nervous systems, on the immunological response, on vasodilation, and on apoptosis.[1] As a consequence, NO-releasing prodrugs, such as organic nitrates and nitroprusside, are often used in the treatment of cardio-circulatory failures. Indeed, a large class of NO-releasing prodrugs is currently employed.[2,3]

NO also plays a crucial role in wound healing processes,[4] provided that the NO production can be increased by the activation of cNOS and by the synthesis of iNOS. In fact, NO modulates cytokine activity in the inflammatory process, in angiogenesis, and in cell proliferation.[5] Hyaluronic acid (HA) is also known to play an important role in the wound healing process. In the context, we wish to report here the synthesis and the characterization of new NO-donors based on HA, using linear and cross-linked derivatives aimed at combining the properties of HA and NO. In such derivatives, spermidine molecules are linked via one primary amino group only to HA (soluble amide derivatives) or via both primary amino groups to different HA chains (cross-linked amide derivatives). The products can readily absorb NO molecules which form specific covalent bonds with the secondary amine groups of sperimidine to yield NONO-ate structures.[6] Subsequently, the latter are able to release NO in solution, at certain values of pH and temperature, with a characteristic kinetics dependent mainly on the degree of substitution/cross-link density of the HA derivatives.

Materials and Methods

Materials. HA sodium salt, from Fidia Advanced Biopolimers (FAB srl, Abano Terme, Padua, Italy) $M\eta = 200$ kDa, was used throughout. Spermidine trihydrochloride salt was supplied by Fluka, Milan, Italy. All other chemicals were reagent grade and were used without further purification.

Synthesis of HA−Spermidine Hydrosoluble Derivative. HA (≈ 200 mg) was dissolved in 8 mL of MES [2-(*N*-morpholino)-ethanesulfonic acid buffer (50 mM, pH = 4); 144 mg of EDC·HCl [*N*-(3-dimethylaminopropyl)-*N*′-ethylcarbodimide hydrochloride)], and 88 mg of NHS (*N*-hydroxysuccinimide) and 1 g of spermidine trihydrochloride salt were added. The reaction was performed at room temperature under stirring for 24 h; the solution was then dialyzed (cutoff = 12 kDa) against a NaCl saturated solution for 1 day and then against distilled water for 5 days. Finally, the solution was freeze-dried.

Synthesis of HA−Spermidine Hydrogels by Ugi's Reaction. Spermidine (≈ 240 mg) trihydrochloride salt was dissolved in 1.2 mL of distilled water to obtain a 784 mM solution. Samples were obtained dissolving 120 mg of HA in 2 mL of distilled water (polymer concentration: 6% w/V). The solutions were acidified with a few drops of HCl 0.5 M to obtain a pH of 4. Different amounts of spermidine solution were added to the samples to obtain networks with a theoretical cross-linking degree (TCD) ranging from 5% up to 25%. TCD is defined as the stoichiometric ratio between the moles of diamine and the moles

* To whom correspondence should be addressed. E-mail: vittorio.crescenzi@uniroma1.it.
† University of Rome "La Sapienza".
‡ Institute of Chemical Methodologies.
§ University of Molise.
⊥ Fidia Farmaceutici SpA.

10.1021/bm050904i CCC: $33.50
Published on Web 03/10/2006

of the carboxylic group of HA. Then, 50 μL of formaldehyde and 100 μL of cyclohexylisocyanide were added to the solutions which were stirred for one minute, and then left at rest overnight. The obtained gels were dialyzed against distilled water for 7 days. Five networks with a TCD equal to 5%, 8%, 12%, 15%, and 25% respectively were obtained.

Swelling Measurements. The swelling capacity of the hydrogels, S_w, is defined as the ratio between the weight of swollen gels (W_s) after extensive dialysis against distilled water and the weight of the dry networks (W_d): $S_w = W_s/W_d$. Freeze-dried networks at different cross-linking degree were swollen in distilled water at 25 °C until constant weight.

NMR in Solution. Samples, ≈ 5 mg, were dissolved in 700 μL of a phosphate buffered (pD = 7) D_2O solution 0.1 M NaCl.

^{1}H and ^{13}C NMR experiments were performed at 27 °C on a Bruker AVANCE AQS 600 spectrometer operating at 600.13 and 150.95 MHz, respectively, and equipped with a Bruker multinuclear, *z* gradient probehead. In all of the ^{1}H spectra, a soft presaturation of the HOD residual signal was applied.[7] ^{1}H and ^{13}C assignments were obtained using ^{1}H−^{1}H COSY, ^{1}H−^{1}H TOCSY, and ^{1}H−^{13}C HSQC experiments with a *z* gradient coherence selection. All 2D experiments were carried out using 1024 data points in the f2 dimension and 512 data points in the f1 dimension; the recycle delay was 1 s. The TOCSY experiment was performed with a spin-lock duration of 80 ms. The HSQC experiment was performed using a coupling constant of 150 Hz. The TOCSY and the HSQC experiments were processed in the phase sensitive mode (TPPI) with 512 × 512 data points.

^{1}H and ^{13}C chemical shifts are reported in ppm with respect to 2,2-dimethyl-2-silapentane-5-sulfonate sodium salt (DSS) used as an internal standard.

Pulsed gradient spin−echo (PGSE) measurements were performed both on a free spermidine and on the HA−spermidine sample; in both cases 1 mg of sample was dissolved in 700 μL of a 0.1 M NaCl phosphate buffered (pD=7) D_2O solution.

PGSE experiments were performed with a pulsed field gradient unit producing a magnetic field gradient in the *z* direction with a strength of 55.4 G cm^{-1}. The stimulated echo pulse sequence using bipolar gradients with a longitudinal eddy current delay was used. The strength of the sine-shaped gradient pulse with a duration of 1.8 ms was logarithmically incremented in 32 steps, from 2% up to 95% of the maximum gradient strength, with a diffusion time of 700 ms and a longitudinal eddy current delay of 25 ms. After Fourier transformation and a baseline correction, the diffusion dimension was processed using the DOSY subroutine of the Bruker Xwinnmr software package.

Solid State NMR. Samples were freeze-dried, finely cut, packed into 4 mm zirconia rotors, and sealed with Kel-F caps. Solid state ^{13}C CP-MAS spectra were performed at 50.13 MHz on a Bruker ASX-200 spectrometer. The spin-rate was 8 kHz. The $\pi/2$ pulse width was 3.5 μs, and the relaxation delay was 3 s; 8000 scans were acquired for each spectrum. The cross-polarization was performed applying the variable spin-lock sequence RAMP−CP-MAS;[8,9] the RAMP was applied on the ^{1}H channel, and during the contact time τ, the amplitude of the RAMP increased from 50 to 100% of its maximum value. This method allows the motional modulation of the carbon and proton coupling caused by spinning the sample at high rate to be overcome.

Experiments performed in the cross-polarization mode with a simultaneous phase inversion (CP−SPI) allowed the different type of carbons to be selectively observed;[10,11] the contact time τ for the cross-polarization was 1 ms, whereas the length of the pulse used for the phase inversion was 24 μs.

Spectra were acquired using 1024 data points in the time domain, zero filled and Fourier transformed. The chemical shift was externally referred to tetramethylsilane (TMS).

Cross-Polarization (CP) Dynamic. The ^{13}C CP-MAS spectra are not quantitative because the intensity of the carbon resonances depends on the CP rates, which can be different for different carbon atoms.[12] The CP rate depends on the number of abundant spins I (protons) near the dilute spin S (carbons) and on their distance from S. The question rises when we wish to obtain a quantitative analysis of the intensity of resonances due to carbon of different types. In simple cases, the problem can be solved by investigating the CP dynamic;[12] the kinetic of the CP dynamic can be analyzed using the two-phase polarization transfer model[13,14] which can be described by the equation

$$\frac{S}{S_0} = \exp\left(-\frac{\tau}{T_{1\rho}^{1H}}\right)\left[1 - s\exp\left(-\frac{\tau}{T_{CHR}}\right) - (1-s)\exp\left(-\frac{3\tau}{2T_{CHR}}\right)\exp\left(-\frac{\tau^2}{2T_{CHD}{}^2}\right)\right] \quad (1)$$

where S_0 is the area of the resonance at the time $\tau = 0$, $T_{1\rho}^{1H}$ is the proton spin−lattice relaxation time in the rotating frame, T_{CHD} is the time constant for the first phase, i.e., CP from covalently bonded protons, T_{CHR} is the time constant for the second phase, i.e., CP from the more remote protons, finally, $(1 - s)/s$ is the ratio between the magnitude of the fast and slow polarization transfer phases (this ratio is also fitted to the experimental data).[15] In homogeneous systems, the spin-diffusion process averages the $T_{1\rho}^{1H}$ values of all carbon resonances; under these circumstances the S_0 values obtained fitting the experimental data to the eq 1 are the "true" areas of the resonances.

Therefore, the CP dynamics were carefully investigated. For all samples, a series of ^{13}C−CP MAS spectra were carried out, with the contact time τ ranging from 0.05 up to 12 ms. The intensity of two selected resonances was reported as a function of the contact time; the $T_{1\rho}^{1H}$ and S_0 values were evaluated.

NONO-ate Bond Formation. Freeze-dried samples were placed into a homemade steel reactor. To remove air and to dry both the reactor and the samples, N_2 was fluxed for 20 min and then pressurized at 5 atm for 4 times. Then, NO was pressurized at 5 atm for 3 days. After purging, N_2 was fluxed again to remove NO traces in the reactor. Finally, samples were collected and stored at −20 °C before the NO release measurements.

NO Release. NO release from the samples was measured by colorimetric Griess assay with an HP 8452A diode array UV−vis spectrophotometer. The Griess solution was prepared by dissolving 500 mg of SULF (sulfanilamide) and 10 mg of NEDD (*N*-(1-naphthyl) ethylenediamine dihydrochloride) in 100 mL of PBS 100 mM, pH = 7.4; 4 mg of the sample was placed in 2.5 mL of Griess solution in a 1 cm quartz cell. The NO release was detected recording the absorbance increase at $\lambda = 496$ nm as a function of time. The concentration of NO released was calculated using the molar absorptivity according to a method reported in the literature (12 500 M^{-1} cm^{-1}).[16]

Scheme 1. Structures of α-Linked and η-Linked HA−Spermidine Water Soluble Derivatives

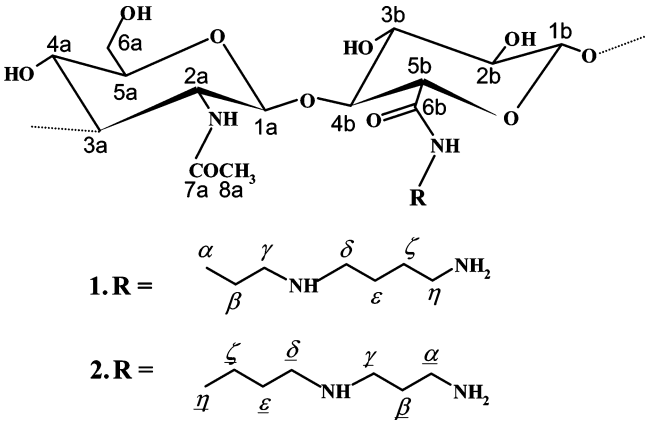

Results and Discussion

Synthesis of Water Soluble HA−Spermidine Derivative. The carboxylic group activation with a water soluble carbodi-

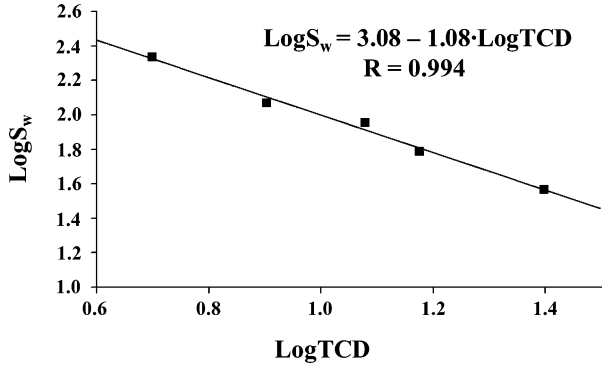

Figure 1. log S_w vs log TCD in water at 25 °C for the HA−spermidine Ugi gels with a TCD equal to 5%, 8%, 12%, 15%, and 25%.

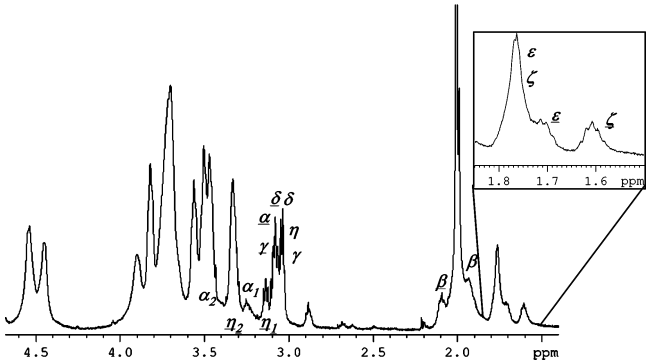

Figure 2. ^{1}H NMR spectrum (600.13 MHz) of HA−spermidine in phosphate buffered (pD=7) D_2O solution 0.1 M NaCl at 27 °C, along with the assignment of the resonances of spermidine bound to HA. In the insert, the resonances used for the quantitative evaluation of the spermidine moieties bound to HA are evidenced.

imide[17] and the subsequent reaction with a primary amine (or diamine) are widely used to obtain HA derivatives.[18] We employed the EDC/NHS system and a large excess of spermidine in order to reduce the probability of cross-links formation.[19−22] The HA−spermidine hydrosoluble product was purified by dialysis and recovered by freeze-drying. Note that a spermidine molecule can be bound to HA in the two possible ways as shown in Scheme 1.

Synthesis of Networks. We used Ugi's reaction[23] to obtain hydrogels from different polysaccharides.[24,25] Because of the rapidity of the Ugi condensation, we used spermidine in its more soluble trihydrochloride form in a 6% w/V HA solution. Gels with different degrees of cross-linking were easily obtained adding different amounts of spermidine solution in H_2O. The cross-linking process lasted a few seconds, that is a time much shorter than the time necessary for the cross-linking of the HA−lysine system.[26] The resulting gels were dialyzed against distilled water for several days and then freeze-dried.

Swelling Measurements. In Figure 1, the swelling data for the HA−spermidine gels with a TCD equal to 5%, 8%, 12%, 15%, and 25% are reported. The log(S_w) vs log TCD plot shows a linear trend. As expected, when the TCD value is increased, the swelling diminishes. Fitting the experimental data to the equation log $S_w = A + B$ log TCD, the parameters A and B are found to be 3.08 and 1.09, respectively. The estimated A and B values for HA−spermidine networks are very similar to those previously found for HA−lysine networks.[26]

NMR in Solution.

NMR Characterization of HA−Spermidine along with the Schemes of a HA−Spermidine Derivatives, namely α and $\underline{\eta}$. Because spermidine is not a symmetric molecule, it is expected to be bound to HA in two possible ways as shown in Scheme 1.

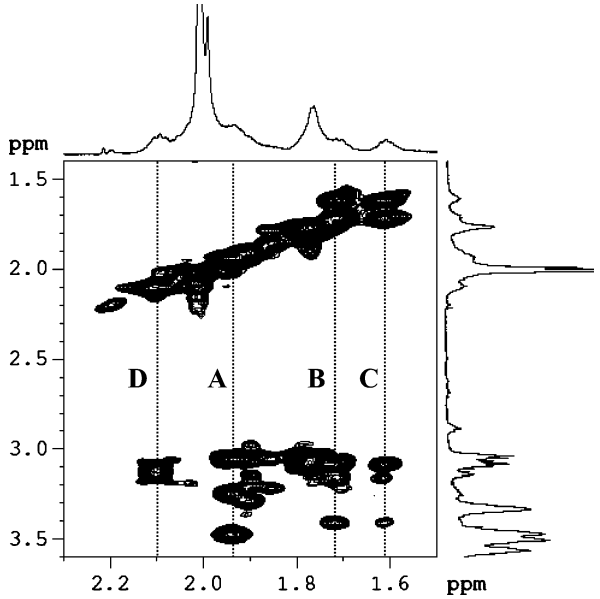

Figure 3. Expansion of ^{1}H−^{1}H TOCSY map of HA−spermidine in phosphate buffered (pD = 7) D_2O solution 0.1 M NaCl at 27 °C. Four spin-systems, A, B, C, and D are evidenced.

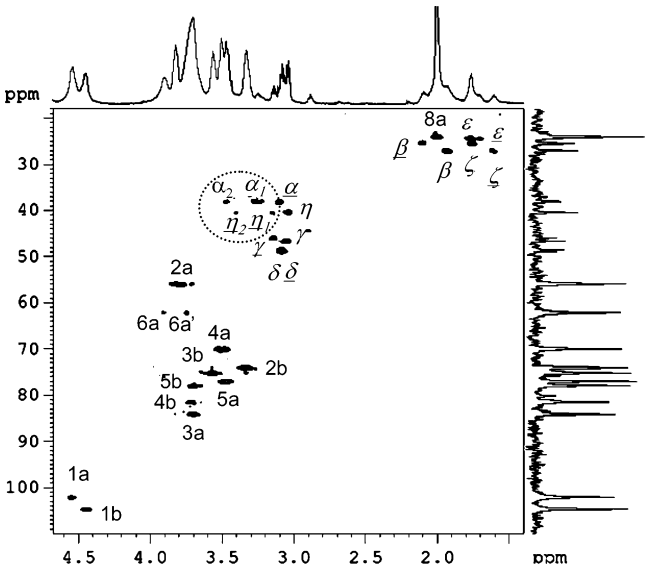

Figure 4. ^{1}H−^{13}C HSQC map of HA−spermidine in phosphate buffered (pD = 7) D_2O solution 0.1 M NaCl at 27 °C. The full assignment is also reported. The ^{1}H and the ^{13}C NMR spectra are reported as projections in the f2 and f1 dimensions, respectively.

The ^{1}H NMR spectrum of HA−spermidine is shown in Figure 2. Besides the resonances of the HA moiety, other resonances are observed. The 2D-TOCSY and the comparison with the ^{1}H spectrum of a standard of spermidine allows the presence of α and $\underline{\eta}$ HA−spermidine derivatives to be revealed, see numbers 1 and 2, respectively, in Scheme 1. Four different spin systems, reported in Figure 3 as A−D, have been identified. The spin system A shows the correlation among the methylene protons α_1, α_2, β, and γ. In fact, after the binding with HA, the methylene protons α both resonating at 3.099 ppm (α′) in free spermidine, become fully nonequivalent and downfield shifted, their chemical shift being at 3.262 and 3.475 ppm, respectively. After the binding, the methylene protons β and γ are both upfield shifted, their chemical shifts being at 1.937 and 3.043

Table 1. ^{1}H and ^{13}C Assignment of HA−Spermidine and Free Spermidine Trihydrochloride Salt in Phosphate Buffered (pD = 7) D_2O Solution 0.1 M NaCl at 27 °C

	^{1}H (ppm)	^{13}C (ppm)
HA−spermidine		
1a	4.543	102.14
2a	3.816	55.89
3a	3.700	84.12
4a	3.490	70.05
5a	3.462	77.12
6a	3.905	62.06
6a′	3.739	62.06
7a		176.04
8a	2.006	24.05
1b	4.446	104.73
2b	3.331	74.10
3b	3.560	75.17
4b	3.716	81.55
5b	3.691	77.94
6b		175.20
α_1	3.262	38.04
α_2	3.475	38.04
β	1.937	27.01
γ	3.043	46.65
δ	3.080	48.49
ϵ	1.775	24.33
ζ	1.756	25.50
η	3.041	40.38
$\underline{\alpha}$	3.100	38.22
$\underline{\beta}$	2.103	25.36
$\underline{\gamma}$	3.130	46.02
$\underline{\delta}$	3.089	48.81
$\underline{\epsilon}$	1.725	24.45
$\underline{\zeta}$	1.625	27.05
$\underline{\eta}_1$	3.166	40.39
$\underline{\eta}_2$	3.410	40.39
free spermidine		
α'	3.099	39.29
β'	2.111	26.42
γ'	3.144	47.14
δ'	3.097	49.69
ϵ'	1.785	25.48
ζ'	1.767	26.64
η'	3.035	41.43

ppm, respectively, being at 2.111 (β') and 3.144 ppm (γ') in free spermidine. The spin system B shows the correlation among protons δ, ϵ, ζ, and η: their chemical shifts are rather unaffected after the binding, these protons being far away from the binding site. Therefore, the spin systems A and B fully match with number 1 in Scheme 1. Two other spin systems are observable in the TOCSY slice of Figure 3. The spin system C shows the correlation among the methylene protons $\underline{\eta}_1$, $\underline{\eta}_2$, $\underline{\zeta}$, $\underline{\epsilon}$, and $\underline{\delta}$. Note that, again, after binding with HA the methylene protons $\underline{\eta}$ both resonating at 3.035 ppm (η') in free spermidine become fully nonequivalent and downfield shifted, being at 3.410 and 3.166 ppm, respectively. The methylene protons $\underline{\zeta}$ are also upfield shifted at 1.625 ppm, being at 1.767 (ζ') in free spermidine. Methylene protons $\underline{\epsilon}$ are slightly upfield shifted from 1.785 (ϵ') to 1.725 ppm, whereas protons $\underline{\delta}$ are rather unaffected. Finally, the spin system D shows the correlation among the methylene protons $\underline{\alpha}$, $\underline{\beta}$, and $\underline{\gamma}$, and all of the chemical shifts of these protons are almost unaffected, these protons being far away from the binding site. The spin systems C and D fully match with number 2 in Scheme 1.

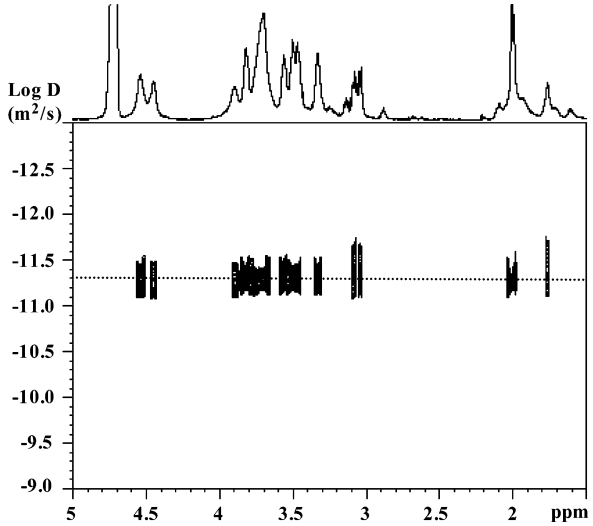

Figure 5. ^{1}H-detected DOSY map of HA−spermidine derivative in phosphate buffered (pD = 7) D_2O solution 0.1 M NaCl at 27 °C. The ^{1}H spectrum is shown as horizontal projection.

To confirm the assignment, an HSQC experiment was also performed (Figure 4). All of the cross-peaks of spermidine are well observable: the unequivalent methylenes α_1 and α_2 as well as the unequivalent methylenes η_1 and η_2 are evidenced. The assignment of all of the other resonances of spermidine bound to HA is also reported in the map.

The assignment of carbon resonances of free spermidine as well as the assignment of carbon resonances of spermidine after the binding with HA are reported in Table 1. For the sake of clarity, the assignment of the resonances of the HA moiety is also reported in the same table; the assignment has been made acting upon literature information[27] and our own data collected using the same solvent as in the actual experiments.

DOSY Measurements. As is well-known from the literature,[28] molecular self-diffusion can be encoded into NMR datasets by means of the pulsed-gradient of the magnetic field (PFG-NMR). Diffusion-ordered NMR spectroscopy (DOSY)[29] is a particularly convenient way of displaying the molecular self-diffusion information in a bi-dimensional array, with the NMR spectrum in one dimension and the self-diffusion coefficient in the other one. DOSY has been successfully used for the analysis of mixtures,[30] for the study of intermolecular interactions,[31,32] for the characterization of aggregates,[33] for the molecular weight determination of uncharged polysaccharides,[34] and for the optimization of the dialysis process of hyaluronic acid derivatives.[35]

As previously shown, TOCSY and HSQC experiments allow a full assignment of the HA−spermidine. The linkage between spermidine and the polymer can be further established by means of a DOSY experiment. Because of the marked difference in the diffusion coefficients, the DOSY map easily establish the presence of spermidine free to move and of spermidine bound to the HA moiety; in fact, after the binding, the diffusion coefficient of the spermidine bound to HA is the same as the one of HA, which is, obviously, much slower than the diffusion coefficient of spermidine free in solution. In fact the diffusion coefficient measured for the HA−spermidine sample was found to be $D = 5.51 \times 10^{-12}$ m^2/s, whereas the diffusion coefficient measured for free spermidine was found to be $D = 1.87 \times 10^{-9}$ m^2/s. Therefore, with the DOSY map, it is also possible to establish the presence, if any, of low molecular weight compounds such as free spermidine, which may impair the

determination of the true percentage of the grafting of spermidine on HA.

Here, we report the DOSY map of the HA−spermidine derivative; the ^{1}H spectrum is shown in the horizontal projection (Figure 5). The map unequivocally demonstrates that all of the resonances of HA as well as of spermidine do show the same diffusion coefficient. The map also indicates that no low molecular weight impurities are present in the sample. The absence of impurities allows the true degree of grafting to be calculated. The degree of grafting, in agreement with Scheme 1, is calculated according to the relationship

$$\text{grafting}\ (\underline{\eta}) = \frac{\frac{I(\underline{\zeta})}{2}}{\frac{I(1_A) + I(1_B)}{2}} = 0.11$$

$I(\underline{\zeta})$ being the area of the signal of the methylene protons $\underline{\zeta}$ resonating at 1.767 ppm, and $I(1_A)$ and $I(1_B)$ the area of the anomeric protons of HA, see the insert in Figure 2.

The degree of grafting, in agreement with Scheme 1, is calculated according to the relationship

$$\text{grafting}(\alpha) = \frac{\frac{I(\underline{\epsilon}) + I(\epsilon) + I(\zeta) - I(\underline{\zeta})}{4}}{\frac{I(1_A) + I(1_B)}{2}} = 0.20$$

where $I(\underline{\epsilon}) + I(\epsilon) + I(\zeta)$ is obtained by integrating the signals of the ^{1}H spectrum resonating between 1.7 and 1.85 ppm (see insert in Figure 2).

The total percentage of grafting is therefore

$$(\text{grafting}(\underline{\eta}) + \text{grafting}(\alpha)) \times 100 = 11\% + 20\% = 31\%$$

^{13}C Solid State NMR. The ^{13}C CP-MAS spectrum of an HA sample is shown in Figure 6a; for the sake of clarity, the assignment of the resonances is also reported[26] in agreement with the labeling shown in Scheme 2.

In the same figure, the spectra of the spermidine-based networks with a different TCD are also shown. Besides the resonances of HA, other resonances are observed in the spectra of the networks; these resonances are due to carbon atoms belonging to the chemical bridges between the HA polymeric chains. Note, however, that the possible presence of spermidine bound as a pendant group cannot be totally disregarded.

The resonance at 168 ppm is due to the amidic carbon 7; the resonance centered at 47 ppm is due to the methine carbon 1 of the cyclohexyl rings and to the methylene carbons γ and δ of spermidine; the resonance at 33 ppm is ascribed to the methylene

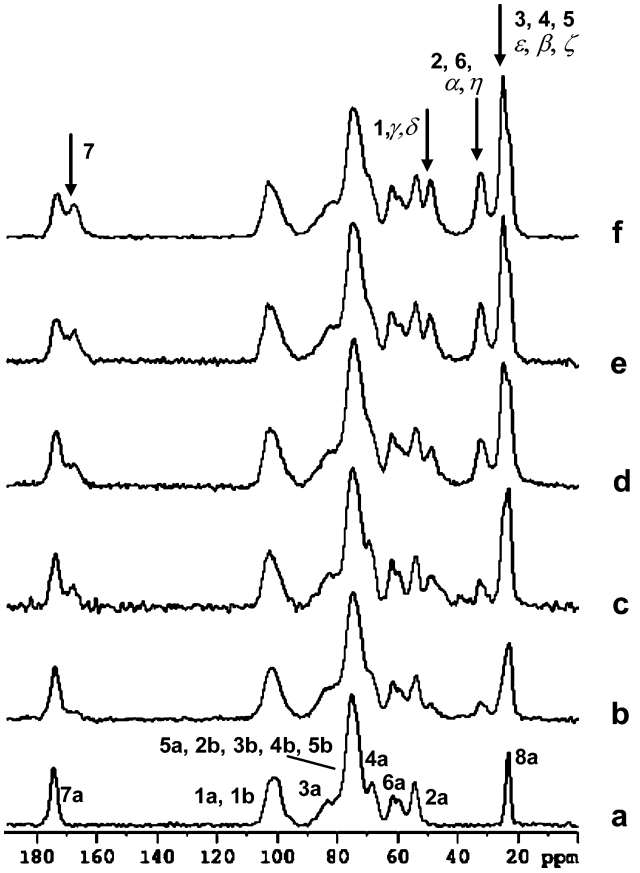

Figure 6. ^{13}C CP-MAS NMR spectra of HA along with the resonance assignment (a); HA−spermidine Ugi networks with TCD = 5% (b), TCD = 8% (c), TCD = 12% (d), TCD = 15% (e), TCD = 25% (f); the assignment of the resonances of the networks is also reported.

carbons 2 and 6 of the cyclohexyl rings and to the methylene carbons α and η of spermidine; finally, methylene carbons 3, 4, and 5 of the cyclohexyl ring and methylene carbons ϵ, β, and ζ of spermidine resonate at about 24 ppm almost fully overlapped to the intense resonance of the acetyl carbon of HA.

To further confirm the assignment of the resonances, the CP−SPI pulse sequence was applied. Using this sequence, a full spectral editing of the CP-MAS spectrum was performed. As a result, a spectrum was obtained where methine carbon resonances are zeroed and methylene carbon resonances are inverted, whereas resonances due to quaternary and methyl carbon atoms are intense and positive, see Figure 7. In this figure, the ^{13}C CP-MAS spectrum (top) of the spermidine-based network with TCD = 25% is compared with the CP−SPI spectrum (bottom) of the same sample. In agreement with the assignment given above, all of the methylene carbons resonances were assigned.

Scheme 2. Structure of HA−Spermidine Ugi Networks

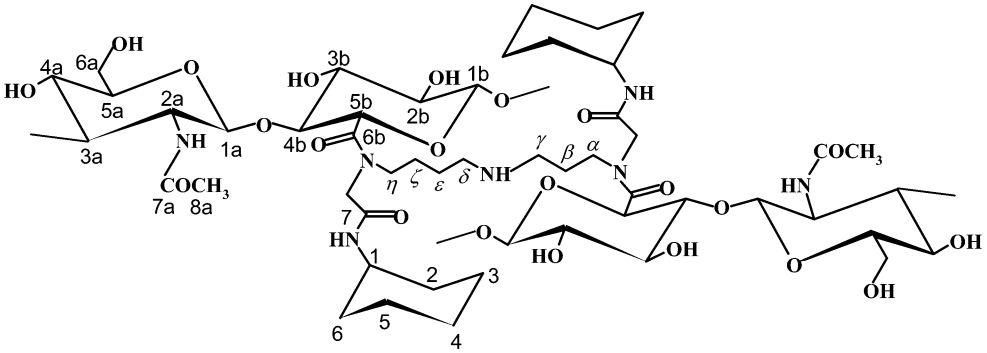

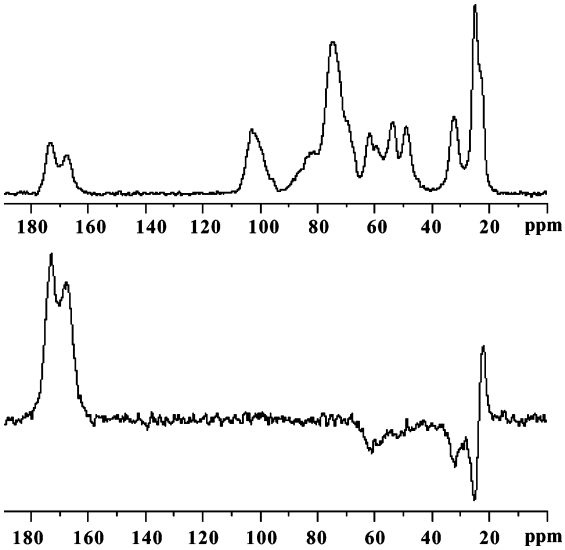

Figure 7. Top: ^{13}C CP-MAS NMR spectrum of HA−spermidine gel with TCD = 25%. Bottom: ^{13}C CP−SPI spectrum of the same sample.

By comparing the spectra of the HA networks reported in Figure 6, a−f, an increment of the intensity of the resonances centered at 24, 33, 47, and 168 ppm is observable; the intensity of these resonances definitely increases as the TCD increases. This trend qualitatively matches with the reported TCD.

The area of the resonance centered at 33 ppm, due to the methylene carbons 2 and 6 of the cyclohexyl rings and to the methylene carbons α and η of spermidine, and the area of the resonance centered at 105 ppm, due to the anomeric carbons of HA, may be used for evaluating the real cross-linking degree (RCD). However, since ^{13}C CP-MAS spectra are not quantitative, caution must be used in the quantitative evaluation of the intensity and/or area of the resonances.[36] Nevertheless, in homogeneous systems, the "true" area of the resonances, S_0, can be obtained fitting the experimental data to eq 1. We recall that in an homogeneous system, the spin diffusion process averages all of the $T_{1\rho}^{1H}$ values. Therefore, the CP dynamic was carefully investigated for all the samples.

^{13}C CP-MAS spectra were run at different contact times, τ, with τ ranging from 0.05 up to 12 ms. The areas of the resonances centered at 105, $S_0(105)$, and 33 ppm, $S_0(33)$, respectively, were reported as a function of the contact time. As an example, the correlation between the area of these resonances and the contact time is shown in Figure 8 for two spermidine-based networks with TDC = 12 (a) and 25 (b), respectively. Fitting the experimental data to eq 1, $T_{1\rho}^{1H}$ and S_0 values were obtained.

The values found for the network with TDC = 25 are

$$S_0(105) = 1.5 \pm 0.2 \; S_0(33) = 0.91 \pm 0.02$$

$$T_{1\rho}^{1H}(105) = (5.4 \pm 0.8) \text{ ms } T_{1\rho}^{1H}(33) = (5.4 \pm 0.3) \text{ ms}$$

whereas the values found for the network with TDC=12 are

$$S_0(105) = 1.7 \pm 0.1 \; S_0(33) = 0.60 \pm 0.01$$

$$T_{1\rho}^{1H}(105) = (5.0 \pm 0.3) \text{ ms } T_{1\rho}^{1H}(33) = (5.4 \pm 0.2) \text{ ms}$$

Because in both samples the selected resonances show the same $T_{1\rho}^{1H}$ values within experimental errors, the samples can be considered as homogeneous systems. As a consequence, the obtained S_0 values can be used to quantitatively evaluate the RCD (real degree of cross-link)

$$\text{RCD} = \frac{\dfrac{S_0(33)}{n}}{\dfrac{S_0(105)}{m}}$$

where $n = 6$ is the number of carbon atoms contributing to the area of the resonance at 33 ppm and $m = 2$ is the number of the anomeric carbon atoms contributing to the area of the resonance at 105 ppm.

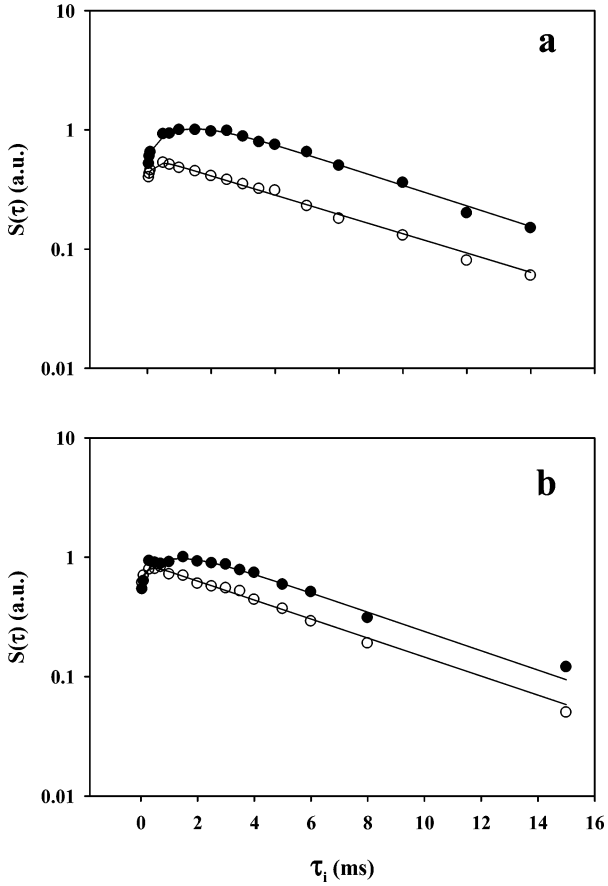

Figure 8. Area of the resonances centered at 105 ppm $S(\tau)$ (●) and 33 ppm $S(\tau)$ (○) reported as a function of the contact time for two spermidine-based networks with TDC = 12% (a) and 25% (b).

Table 2. TCD Values of the Spermidine-based Networks Compared with the RCD Values as Obtained from Solid State NMR

TCD (%)	RCD (%)
25	20.0 ± 0.5
15	13.0 ± 0.4
12	11.8 ± 0.4
8	8.0 ± 0.5
5	4.9 ± 0.4

In Table 2, the TCD values of the spermidine-based networks are compared with the RCD values obtained from NMR data; the error on the RCD percentage was calculated applying the error propagation theory.

NO Release. NONO-ate bond formation on secondary amine after incubation under NO pressure, see Scheme 3, is largely described in the literature.[37,38]

Scheme 3. Schematic Representation of NONO-ate Bond Formation on Secondary Amine after Incubation under NO Pressure and Subsequent NO Release in Physiological Conditions

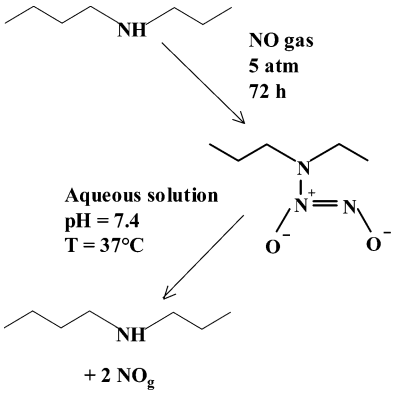

To obtain covalent linking of NO on HA−spermidine water soluble and cross-linked derivatives, samples were treated with NO at 5 atm in a steel reactor for 72 h. Due to the high reactivity of NO with water to give very corrosive nitrous acid, it is important to purge the reactor with dry N_2 or Ar to eliminate moisture from the reactor and the samples.

Furthermore, due to the sensitivity of the NONO-ate bond to temperature, samples have to be stored at −20 °C before NO-release monitoring.

A variety of analytical procedures to monitor nitric oxides in air or in solution have been widely used, as chemometric,[39] electrochemical,[40] spectrometric (EPR),[41] or spectrophotometric methods.[42,43] A simple and useful procedure is the Griess colorimetric assay in aqueous solution[16] that uses the nitrosation of sulfanilamide in the presence of *N*-(1-naphthyl) ethylenediamine dihydrochloride to give an orange-colored azo-compound. The quantity of NO released from the samples and reacting with Griess reagents is easily monitored with an UV−vis spectrophotometer at $\lambda = 496$ nm.

The experiments on HA−spermidine water soluble or cross-linked derivatives were performed at the same concentration, 1.6 mg/mL, in the Griess solution at physiological values of pH and temperature. The increase of the absorbance at $\lambda = 496$ nm vs the time for a water soluble sample and for all the cross-linked gels is reported in Figures 9 and 10, respectively.

All samples show NO release. Absorbance values are transformed into NO concentration (μM) using the molar absorptivity value $\epsilon = 12\,500\ M^{-1}\ cm^{-1}$ reported in the literature for the same experimental conditions.[16] The assay is both sensitive and linear over the range of values observed.

The water soluble derivative shows a complete gas release

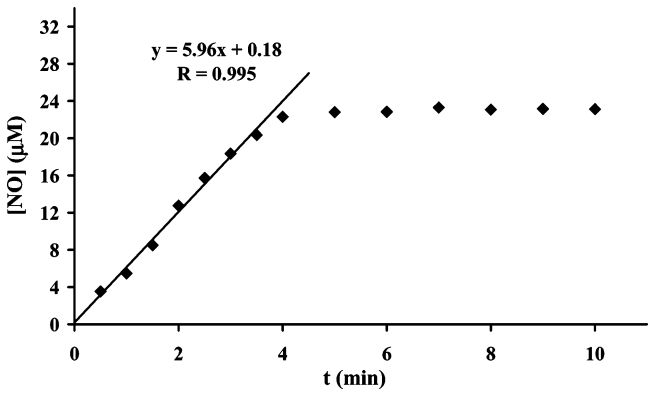

Figure 9. Kinetic of NO-release from HA−spermidine in a Griess phosphate buffered solution 0.1 M (pH = 7.4) at $T = 37$ °C.

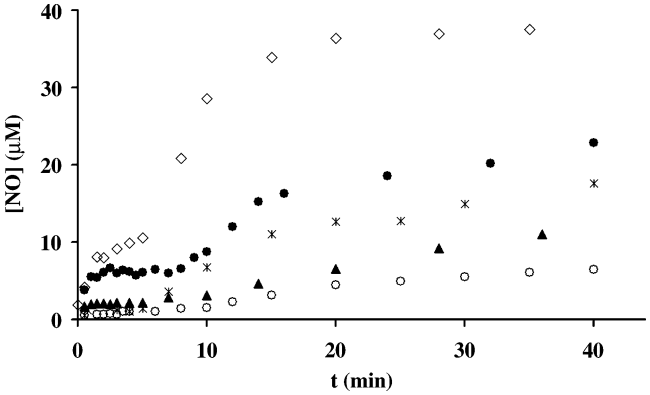

Figure 10. Kinetics of NO-release from HA−spermidine gels with different TCD in a Griess phosphate buffered solution 0.1 M (pH = 7.4) at $T = 37$ °C: TCD = 25% (◇), TCD = 15% (●), TCD = 12% (*), TCD = 8% (▲), TCD = 5% (○).

in about 4 min, with an initial linear trend pointing to a zero order kinetic (Figure 9).

NO release from the Ugi networks, re-swollen as gels in aqueous media, shows more complex kinetics (Figure 10). A rather fast increase of the absorbance is observed in the first few seconds, and then for several minutes, a slow increase of the absorbance is observed. Finally, a pseudolinear trend prevails until the complete gas loss is reached. This behavior can be explained considering the nonsoluble gel structure: the NO molecules closer to the surface are, in fact, quickly released in solution, whereas the NO molecules inside the bulk of the gel are slowly released. Therefore, the whole process depends on the swelling of the gels, as well as on the diffusion of the Griess reagents inside and outside the gel bulk. A qualitative explanation of the increase in the amount of NO released with increasing degree of gels cross-linking may be made considering that the higher the TCD, the higher the number of NO-binding sites in the gels.

Conclusions

New NO donors based on hyaluronic acid derivatives with modulable NO-release properties in physiological conditions have been synthesized and structurally characterized. To form NONO-ate structures able to release NO in solution, we used spermidine as the amine linking agent. The water soluble derivative of HA and spermidine was obtained by amidation reaction in aqueous media using EDC/NHS activation of the HA carboxylate. The HA−spermidine derivative was fully characterized by ^1H and ^{13}C NMR spectroscopy in solution. The degree of grafting of spermidine on HA was also obtained.

The cross-linked derivatives of HA were synthesized by Ugi's reaction using formaldehyde, cyclohexylisocyanide and spermidine as diamine. The resulting networks having different cross-linking degrees were studied by ^{13}C CP-MAS NMR spectroscopy. Furthermore, the study of the cross-polarization dynamic process allowed the degree of cross-linking to be quantitatively ascertained.

The HA−spermidine hydrogels were incubated in NO gas under pressure to obtain the NONO-ate bond formation involving the secondary amine groups of the spermidine residues. The kinetic of the NO-release from the diazeniumdiolate structures was monitored in aqueous solution under physiological conditions using the colorimetric Griess assay. Soon, the potential of the novel HA derivatives for therapeutic formulations will be ascertained by means of in vivo experiments, especially in

wound healing processes in which both NO and hyaluronan play important roles.

Acknowledgment. This work has been carried out with the financial support of Fidia Farmaceutici, Abano Terme (PD), Italy.

References and Notes

(1) Wink, D. A.; Mitchell, J. B. *Free Radical Biol. Med.* **1998**, *25* (4−5), 434−456.
(2) Wang, P. G.; Xian, M.; Tang, X.; Wu, X.; Wen, Z.; Cai, T.; Janczuk, A. J. *Chem. Rev.* **2002**, *102*, 1091−1134.
(3) Napoli, I.; Ignarro, L. J. *Annu. Rev. Pharmacol. Toxicol.* **2003**, *43*, 97−123.
(4) Frank, S.; Kämpfer, H.; Wetzler, C.; Pfeilschifter, J. *Kidney Int.* **2002**, *61*, 882−888.
(5) Schwentker, A.; Vodovotz, Y.; Weller, R.; Billiar, T. R. *Nitric Oxide* **2002**, *7*, 1−10.
(6) Hrabie, J. A.; Keefer, L. K. *Chem. Rev.* **2002**, *102*, 1135−1154.
(7) Guerènon, M.; Plateu, P.; Decorps, M. *Prog. NMR Spectrosc.* **1991**, *23*, 135−109.
(8) Metz, G.; Wu, X.; Smith, S. O. *J. Magn. Reson. A* **1994**, *110*, 219.
(9) Cook, R. L.; Langford, H. H.; Yamadagni, R.; Preston, C. M. *Anal. Chem.* **1996**, *68*, 3979.
(10) Wu, X.; Zilm, K. W. *J. Magn Reson.* **1993**, *A102*, 205.
(11) Wu, X.; Zilm, K. W. *J. Magn Reson.* **1993**, *A104*, 119.
(12) Voelkel, R. *Angew. Chem., Int. Ed. Engl.* **1988**, *27*, 1468−1483.
(13) Ha, M. A.; Evans, B. W.; Jarvis, M. C.; Apperley, D. C.; Kenwright, A. M. *Carbohydr. Res.* **1996**, *288*, 15−23.
(14) Wu, X.; Zhang, S. *Phys. Rev B* **1988**, *37*, 9827−9829.
(15) Jarvis, M. C.; Fenwick, K. M.; Apperley, D. C. *Carbohydr. Res.* **1996**, *288*, 1−14.
(16) Nims, R. W.; Darbyshire, J. F.; Saavedra, J. E.; Christodoulou, D.; Hanbauer, I.; Cox, G. W.; Grisham, M. B.; Laval, F.; Cook, J. A.; Krishna, M. C.; Wink, D. A. *Methods: Compan. Methods Enzymol.* **1995**, *7*, 48−54.
(17) Tomihata, K.; Ykada, Y. *J. Biomed. Mater. Res.* **1997**, *37* (2), 243−251.
(18) Crescenzi, V.; Francescangeli, A.; Renier, D.; Bellini, D. *Biopolymers* **2002**, *64* (2), 86−94.
(19) Bulpitt, P.; Aeschlimann, D. *J. Biomed. Mater. Res.* **1999**, *47* (2), 152−169.
(20) Pouyani T.; Kuo, J.; Harbison G.; Prestwich, G. *J. Am. Chem. Soc.* **1992**, *114* (15), 5972−5976.
(21) Kuijpers, A. J.; Engbers, G.; Feijen, J.; De Smedt, S.; Meyvis, T.; Demeester, J.; Krijgsveld, J.; Zoat, S. A. J.; Dankert, J. *Macromolecules* **1999**, *32* (10), 3325−3333.
(22) Park, S.; Park, J.; Kim, H. O.; Song, M. J.; Suh, H. *Biomaterials* **2002**, *23* (4), 1205−1212.
(23) Ugi, I.; Lohberger, S.; Karl, R. The Passerini and Ugi reactions. In *Comprehensive organic synthesis*; Trost, B. M., Fleming, I., Eds.; Pergamon Press: London, 1991; Vol. II, pp 1086−1109.
(24) de Nooy, A. E. J.; Masci, G.; Crescenzi, V. *Macromolecules* **1999**, *32*, 1318−1320.
(25) de Nooy, A. E. J.; Capitani, D.; Masci, G.; Crescenzi, V. *Biomacromolecules* **2000**, *1* (2), 259−267.
(26) Crescenzi, V.; Francescangeli, A.; Capitani, D.; Mannina. L.; Renier, D.; Bellini, D. *Carbohydr. Polym.* **2003**, *53*, 311−316.
(27) Cowman, M. K.; Hittner, D. N.; Feder-Davis, J. *Macromolecules* **1996**, *29*, 2894−2902.
(28) Stejskal, E. O.; Tanner, J. E. *J. Chem. Phys.* **1965**, *42*, 288−292.
(29) Morris, K. F.; Johnson, C. S. *J. Am. Chem. Soc.* **1992**, *114* (8), 3139−3141.
(30) Morris, K. F.; Stilbs, P.; Johnson, C. S. *Anal. Chem.* **1994**, *66*, 211−215.
(31) Kapur, G. S.; Cabrata, E. J.; Berger, S.; *Tetrahedron Lett.* **2000**, *41*, 7181−7185.
(32) Viel, S.; Mannina, L.; Segre, A. L. *Tetrahedron Lett.* **2002**, *43* (14), 2515−2519.
(33) Morris, K. F.; Johnson, C. S. *J. Am. Chem. Soc.* **1993**, *115*, 4291−4299.
(34) Viel, S.; Capitani, D.; Mannina, L.; Segre, A. L. *Biomacromolecules* **2003**, *4*, 1843−1847.
(35) Crescenzi, V.; Francescangeli, A.; Taglienti, A.; Capitani, D.; Mannina, L. *Biomacromolecules* **2003**, *4*, 1045−1054.
(36) Harris, R. K. In *Multinuclear Magnetic Resonance in Liquids and Solids- Chemical Application*; Granger, P., Harris, H. K., Eds.; NATO ASI Series 322; Kluwer: Dordrecht, The Netherlands, 1988; p 291.
(37) Drago, S.; Paulik, F. E. *J. Am. Chem. Soc.* **1960**, *82* (1), 96−98.
(38) Drago, R. S.; Ragsdale, R. O.; Eyman D. P. *J. Am. Chem. Soc.* **1961**, *83*, 3 (21), 4337−4339.
(39) Beckman, J. S.; Conger, K. A. *Methods: Compan. Methods Enzymol.* **1995**, *7*, 35−39.
(40) Wink, D. A.; Christodoulou, D.; Ho, M.; Krishna, M. C.; Cook, J. A.; Haut, H.; Randolph, J. K.; Sullivan, M.; Coia, G.; Murray, R.; Meyer, T. *Methods: Compan. Methods Enzymol.* **1995**, *7*, 71−77.
(41) Venkataraman, S.; Martin, S. M.; Schafer, S. Q.; Buettner, G. R. *Free Radical Biol. Med.* **2000**, *29* (6), 580−585.
(42) Kudo, S.; Bourrassa, J. L.; Boggs, S. E.; Sato, Y.; Ford, P. C. *Anal. Biochem.* **1997**, *247*, 1193−202.
(43) Miles, A. M.; Chen, Y.; Owens, M. W.; Grisham, M. B. *Methods: Compan. Methods Enzymol.* **1995**, *7*, 40−47.

BM050904I